Separation Science and Technology
Publication details, including instructions for authors and subscription information:
http://www.informaworld.com/smpp/title~content=t713708471

A New Composite Sorbent for Methane-Nitrogen Separation by Adsorption

M. S. A. Baksh[a]; A. Kapoor[a]; R. T. Yang[a]
[a] DEPARTMENT OF CHEMICAL ENGINEERING, STATE UNIVERSITY OF NEW YORK AT BUFFALO, BUFFALO, NEW YORK

To cite this Article Baksh, M. S. A. , Kapoor, A. and Yang, R. T.(1990) 'A New Composite Sorbent for Methane-Nitrogen Separation by Adsorption', Separation Science and Technology, 25: 7, 845 — 868
To link to this Article: DOI: 10.1080/01496399008050370
URL: http://dx.doi.org/10.1080/01496399008050370

SEPARATION SCIENCE AND TECHNOLOGY, 25(7 & 8), 845-868, 1990

A New Composite Sorbent for Methane-Nitrogen Separation by Adsorption

M. S. A. BAKSH, A. KAPOOR, and R. T. YANG*

DEPARTMENT OF CHEMICAL ENGINEERING
STATE UNIVERSITY OF NEW YORK AT BUFFALO
BUFFALO, NEW YORK 14260

Abstract

Composite sorbents were prepared by depositing molybdenum dioxide on Super A activated carbon. The adsorption isotherms of CH_4 and N_2 were measured. The adsorption capacities and BET surface areas of these adsorbents decreased with an increase in the amount of MoO_2; however, the equilibrium selectivity ratio (CH_4/N_2) increased significantly. Therefore, an optimum quantity of MoO_2 should be used to produce a sorbent with high adsorption capacity and selectivity ratio (CH_4/N_2). An adsorbent containing 18.2 wt% MoO_2 was found to be optimum which showed a CH_4/N_2 selectivity ratio of 4.25. The selectivity ratio decreased with pressure, and leveled off to about 3 at 12 atm. The separation of a CH_4/N_2 (50/50) mixture by pressure swing adsorption (PSA) was studied by using an equilibrium model. A new PSA cycle is described by which pipeline quality methane (>90% CH_4 purity) could be produced using the composite sorbent at a recovery of 73% and a throughput of 200 L STP/h/kg.

INTRODUCTION

Due to the high N_2 content (above 10% by volume), much of the natural gas resources are not readily usable. The natural gas used commercially must have at least 90% CH_4. Moreover, the N_2 content increases with time after the reservoir is in service (*1*). Presently, costly cryogenic separation is the most economic commercial means for CH_4/N_2 separation. However, adsorption separation processes may compete with the cryogenic process if a suitable sorbent is available commercially. Presently no adsorbents have been developed for CH_4/N_2 separation.

*To whom correspondence should be addressed.

In the first part of the paper, a new adsorbent which possesses a high selectivity for CH_4 is described. The sorbent was prepared by impregnation of MoO_2 on a commercial activated carbon. The second part is a report of the mathematical modeling results of a pressure swing adsorption (PSA) process using the new composite sorbent. A new PSA cycle is described by which, along with the new sorbent, a CH_4 product containing >90% CH_4 purity is obtained from a 50/50 mixture of CH_4/N_2 at a throughput of 200 L STP/h/kg.

SYNTHESIS OF SORBENT

Samples of MoO_2/activated carbon were prepared by impregnation with aqueous solutions of ammonium heptamolybdate. The activated carbon was the Super A carbon (*2*), produced by Anderson Development Co. All chemicals were of ACS grades. The loadings of MoO_2 were in the range of 8 to 38 wt% as determined by the weight of ammonium heptamolybdate used in the synthesis and the stoichiometry of the decomposition reaction that produced MoO_2. The steps in the synthesis included dissolving the equivalent amount of ammonium heptamolybdate required for a particular loading into a volume of deionized water slightly greater than the cumulative pore volume of the carbon. The activated carbon was added to this aqueous solution and mixed thoroughly into a paste. The resulting mixture was dried in air at 100°C for 4 h. The dried sample was transferred into a ceramic boat that was then placed inside a tube that was heated in a tube furnace. One end of the furnance tube was connected to a N_2 source, and the other end to a vent leading to a fume hood. Nitrogen gas was allowed to flow over the sample inside the tube to purge the system free of air. An inert atmosphere was required before any high temperature heating was carried out to avoid oxidation of the carbon. After purging the system with N_2 for 2 h, the tube furnace was activated, a programmed heating rate of 100°C/h was established to a final temperature of 500°C, and the sample was allowed to soak for 20 h. The furnace was then cooled to room temperature in flowing nitrogen, and the sample was removed and stored in capped vials. The above steps were repeated for different loadings of MoO_2, as well as for the as-received carbon. The BET surface area measured before and after the thermal treatment for the as-received carbon (Sample I, zero MoO_2 loading) confirmed that none of the carbon was oxidized. In this study, MoO_2 loadings of 8.9, 18.2, and 37.2 wt% were obtained, and will be referred to as Samples II, III, and IV, respectively.

SORBENT CHARACTERIZATION AND ADSORPTION ISOTHERMS

X-ray diffraction powder patterns were obtained to identify the crystals of the supported metal oxide(s). The XRD pattern of Sample I showed no peak at $2\theta = 26°$ (with a CuK_α source), indicating no graphitization had occurred in the carbon support. The XRD pattern of Sample III is shown in Fig. 1, along with the diffraction lines [from NBS Standards File (*3*)] of MoO_2 crystal. It is seen that the supported metal oxide was entirely MoO_2.

The surface areas were measured with a Quantasorb Surface Area Analyzer (Quantachrome Corp.). For the measurement of adsorption isotherms, TGA (using a Mettler TA 2000C Thermoanalyzer) was used for

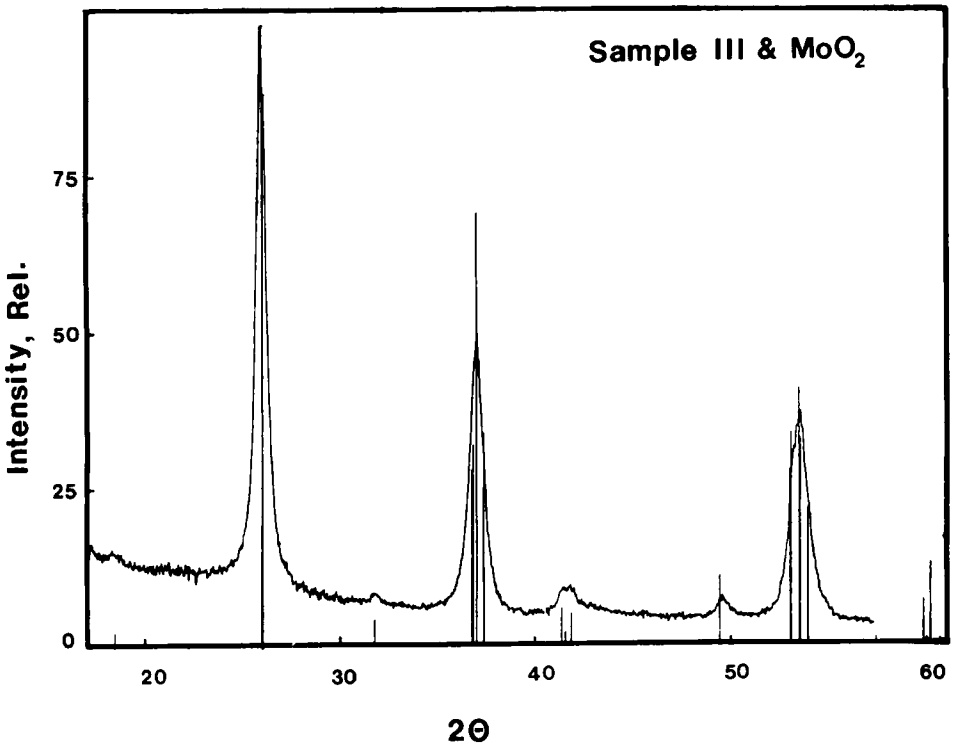

FIG. 1. X-ray powder diffraction pattern of Sample III, superimposed with lines for MoO_2

pressures of 1 atm and below, and a static volumetric system was used for pressures above 1 atm. The gases were supplied by Cryogenic Supply, and the purity specifications were methane (99.0%), carbon dioxide (99.99%), and nitrogen (99.99%). Each of the gases was passed through a molecular sieve (Linde 5A) to ensure the removal of any traces of water and other impurities. The molecular sieve was periodically regenerated by heating at 350°C for about 20 h under vacuum. Prior to surface area and isotherm measurements, each sample was outgassed at 100°C for 15 h. N_2 desorption isotherms at 77 K were used in the surface area analysis. Both BET and Langmuir isotherms were used for surface area calculations. From the same data, the limiting pore volumes (for micropore filling) were calculated from the Dubinin-Radushkevich (DR) equation.

The BET and Langmuir surface areas of the four samples are given in Table 1. The surface areas of a powder MoO_2 sample, which was also included in CH_4 and N_2 adsorption isotherm measurements, are also given in Table 1. In addition, the micropore volumes calculated from the DR equation are listed. The high "surface area" of the Super A carbon, i.e., over 3000 m^2/g, simply indicates that the BET and Langmuir isotherms are not applicable to this carbon. As a basis for comparison, the surface area of separate graphite sheets is 2630 m^2/g. The large "micropore volume" of 1.68 cm^3/g calculated from the DR equation, however, indicates that this carbon contains a large volume of voids which results in large adsorption capacities.

The adsorption isotherms at two temperatures in the four sorbent samples are given in Figs. 2 and 3, respectively, for CH_4 and N_2. These are the TGA results measured at pressures below 1 atm. Isotherms of CH_4 and N_2 at 25°C for Samples I to III at higher pressures (up to 12 atm) are given in Fig. 4. From these results it is seen that the adsorption capacities for both CH_4 and N_2 decreased as the amount of MoO_2 impregnation was increased, i.e., from Sample I to Sample IV. The CH_4 capacity, however, remained relatively high as compared to the commercial sorbents. For example, the CH_4 capacity for Sample III at 1 atm and 25°C was 17.0 cm^3 STP/g for BPL activated carbon and 15.0 cm^3 STP/g for 4A zeolite.

The important result is, however, that the selectivity toward CH_4 was increased by MoO_2 impregnation. The selectivity ratio, expressed as the amount adsorbed CH_4/amount adsorbed N_2, is shown as a function of pressure in Fig. 5 for Samples I-III. The same ratios at 1 atm pressure are also given in Table 1. The selectivity ratio for CH_4/N_2 on the pure MoO_2 powder was 14.04, also given in Table 1. This selectivity ratio is substantially higher than those of the impregnated samples.

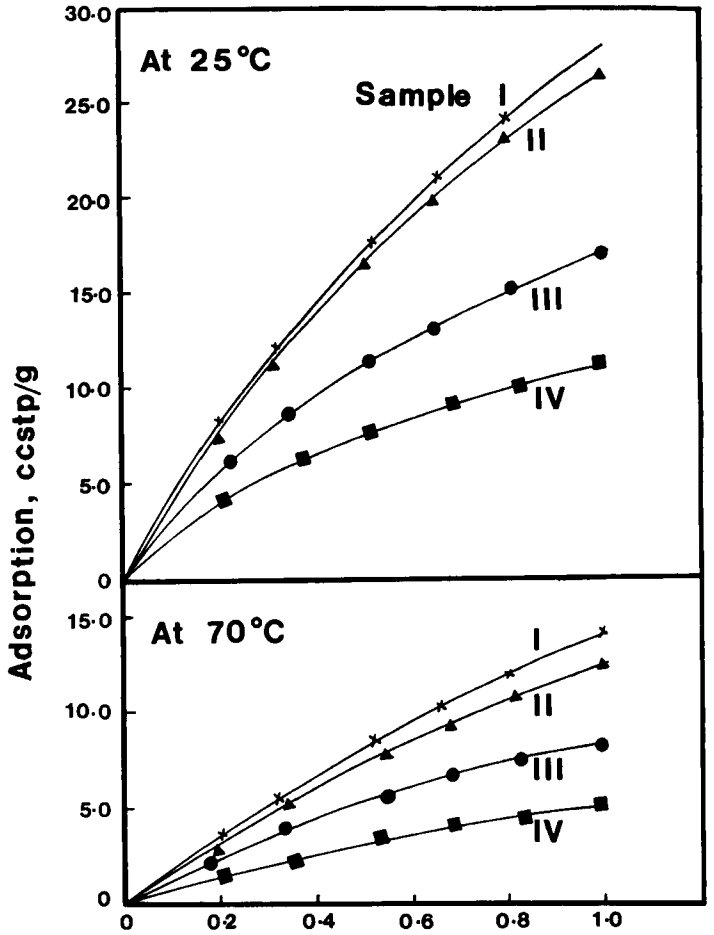

FIG. 2. Adsorption isotherms for CH_4.

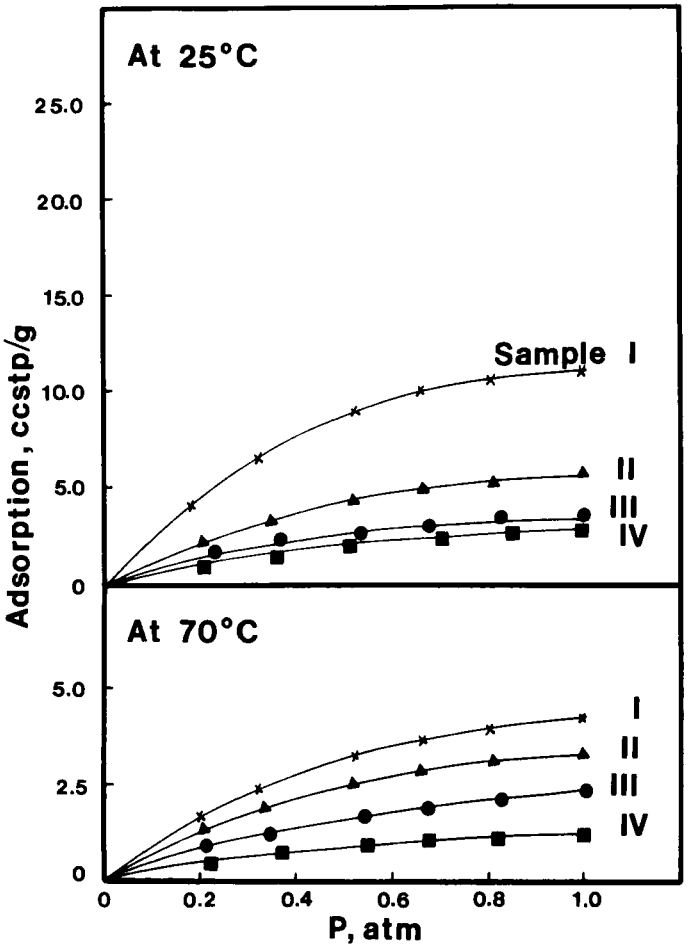

FIG. 3. Adsorption isotherms for N_2.

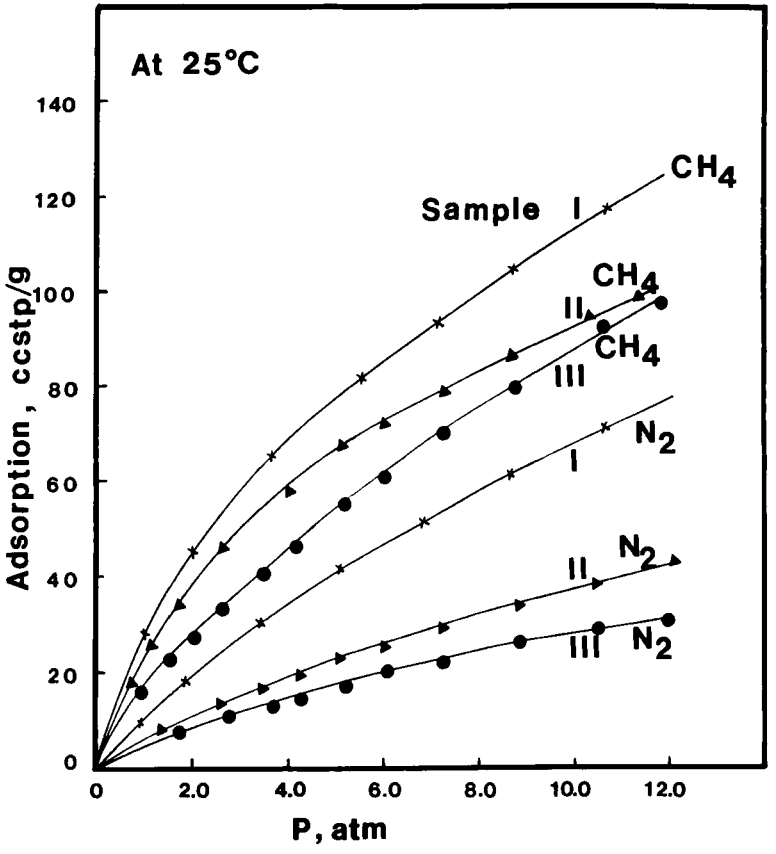

FIG. 4. Adsorption isotherms for CH_4 and N_2 at 25°C.

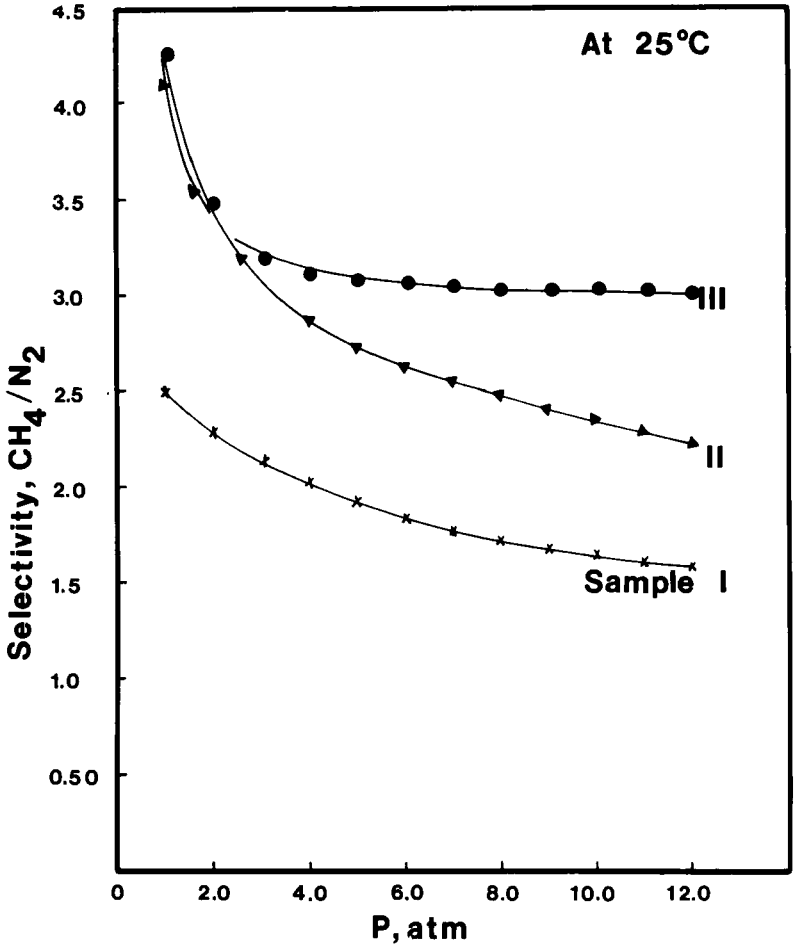

FIG. 5. Adsorption selectivity ratio for CH_4/N_2 at 25°C.

TABLE 1
BET and Langmuir Surface Areas (from N_2 desorption at 77 K), Micropore Volume (from DR equation) and Adsorption Selectivity (at 298 K and 1 atm)

Sorbent	Wt% MoO_2	BET area (m^2/g)	Langmuir area (m^2/g)	Micropore volume (cm^3/g)	CH_4/N_2 selectivity
Sample I	0.00	3004	3338	1.68	2.50
Sample II	8.90	2138	2375	1.19	4.56
Sample III	18.20	1330	1477	0.77	5.00
Sample IV	37.20	832	924	0.49	3.72
MoO_2	100.00	2.94	3.27	—	14.04

The above results indicate that the increase in the selectivity ratio by MoO_2 impregnation was caused by covering the carbon surfaces and micropore with MoO_2. If the total amount adsorbed is the sum of the amounts adsorbed by MoO_2 and uncovered carbon, 22% of the surfaces/micropores in Sample III was covered by MoO_2, with 78% being uncovered carbon. From this simplified picture and assuming that the MoO_2 was dispersed as spherical islands, the diameter of the islands would be approximately 6 Å. This estimate indicates that the MoO_2 was highly dispersed, perhaps due to the strong interactions with the surface oxide groups on carbon. Further increasing the MoO_2 amount from 18.2% (in Sample III) to 37.2% (in Sample IV) only decreased in the selectivity and the adsorption capacity. This result indicates that more pore-blocking than surface-covering took place upon a further increase in MoO_2. The MoO_2 content in Sample III appears to be the optimal amount.

PRESSURE SWING ADSORPTION (PSA) CYCLES

Many PSA cycles have been developed since its invention in the 1950s. These cycles have been reviewed by Yang (*4*), Tondeur and Wankat (*5*), and Sircar (*6*). The basic steps in a PSA cycle are pressurization, adsorption, and depressurization. The main differences among the various PSA cycles are in the pressurization and depressurization steps. The pressurization step can be accomplished either by the feed mixture or by the light component product from another bed. The depressurization can be

accomplished in many ways: countercurrent depressurization (*7*), cocurrent blowdown followed by countercurrent depressurization (*8–10*), and cocurrent heavy component purge followed by countercurrent depressurization (*11–13*). The last option involves purge (or rinse) by the heavy component in the direction of and at the pressure of feed. This step was first suggested by Tamura (*14*) and later commercialized for air separation (*15*).

The PSA cycle used here consists of the following steps.

Step I: Light component (N_2) pressurization
Step II: High pressure adsorption
Step III: Cocurrent heavy component (CH_4) purge
Step IV: Countercurrent evacuation

This cycle will be referred to here as Cycle 1. In Step I the bed is pressurized to the feed pressure (P_H) by the N_2 product from another bed going through Step II. In Step II the high pressure feed flows through the bed while a part of the effluent is used to pressurize another bed, and the rest is collected as N_2 product. Step III, cocurrent heavy component purge, involves purge by the effluent (CH_4 product) from another bed going through Step IV. The effluent from Step III is also collected as N_2 product. Countercurrent evacuation, Step IV, produces effluent rich in CH_4 and is collected as CH_4 product. Step IV also regenerates the bed for the next cycle.

Typically, two or more beds are operated together, so that continuous feed and product are possible. However, since all beds go through identical steps and display identical behavior, only one bed is used in the simulation. The performance of a PSA process is determined by three separation results: product purity, product recovery, and throughput, all at cyclic steady state. The effluents from Steps II and III are collected as N_2 product, whereas the effluent from Step IV is collected as CH_4 product. The N_2 product purity is then defined as the volume averaged concentration over the effuent from Steps II and III, and CH_4 product purity is the volume averaged concentration over the effluent from Step IV. The product purities are expressed as mol%. The products recoveries are defined as

$$N_2 \text{ recovery} = \frac{(N_2 \text{ in Steps II and III effluents}) - (N_2 \text{ used in Step I})}{(N_2 \text{ in feed in Step II})} \times 100$$

and

$$\text{CH}_4 \text{ recovery} = \frac{(\text{CH}_4 \text{ in Step IV effluent}) - (\text{CH}_4 \text{ used in Step III})}{(\text{CH}_4 \text{ in feed in Step II})} \times 100$$

PSA MODEL

A model has been developed to simulate an adsorber bed going through various PSA cycle steps. The model is based on the following assumptions: No variation exists in the radial direction for both concentration and temperature, the flow pattern is described by a plug flow model, mass transfer resistance is negligible, the axial pressure gradient is negligible, and the ideal gas law applies. The model equations have been given elsewhere (*9, 11*). The initial and boundary conditions are similar to those described earlier (*9, 11*) except for the boundary conditions for the pressurization (Step I) and cocurrent heavy component purge (Step III) steps. The boundary conditions for Steps I and III are given as

$$\begin{aligned} &\text{Step I at} && Z = L \text{ (product end)} \\ &&& y_i = y_{i,\text{Pr}} \\ &&& T = T_0 \\ &\text{and at} && Z = 0 \text{ (feed end)} \\ &&& u = 0 \\ &&& P = P(t) \end{aligned}$$

where $y_{i,\text{Pr}}$ is the concentration of the nitrogen product obtained in Step II from another bed.

$$\begin{aligned} &\text{Step III at} && Z = 0 \\ &&& y_i = y_{i,\text{IV}} \\ &&& u = u_{\text{Pu}} \\ &&& T = T_0 \\ &&& P = P_H \text{ (see Fig. 8)} \end{aligned}$$

where $y_{i,\text{IV}}$ is the concentration of the methane product from another bed. The pressure history $P(t)$ is an input variable. For the sake of simplicity, straight line pressure histories are assumed in the pressure-changing steps (Steps I and IV) as shown in Fig. 6. The product concentrations obtained in Steps II and IV are a function of time; however, to make the model

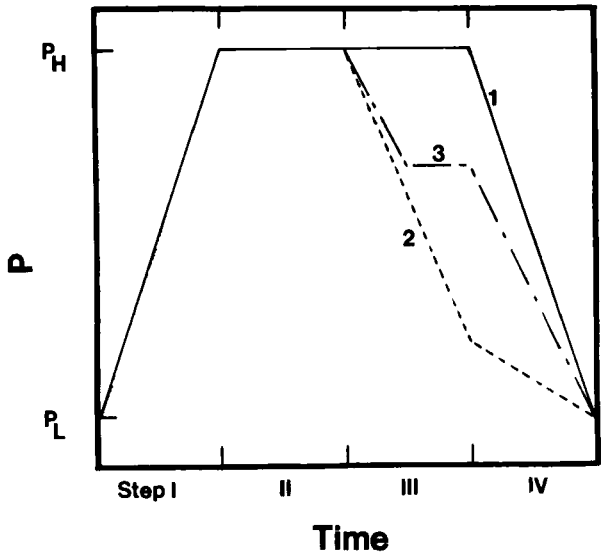

FIG. 6. Pressure histories for various cycles. The numbers on the curves refer to the cycles.

mathematically simpler, average values of the products concentrations are used as boundary conditions in Steps III and I, i.e., $y_{i,IV}$ and $y_{i,Pr}$, respectively. This simplification allows simulation of one bed of the multibed process by taking $y_{i,IV}$ and $y_{i,Pr}$ as the average concentrations from the previous cycle. Thus, for the first cycle, $y_{i,IV}$ is taken as pure methane. The model equations are solved by an implicit backward finite difference scheme.

The initial conditions for each step are the conditions (concentration and temperature profiles in the bed) at the end of the preceding step. The computation is continued until a cyclic steady-state is reached. A process is said to have reached a cyclic steady-state when there is no appreciable change in concentration and temperature profiles in the bed in the corresponding steps from cycle to cycle.

PSA SIMULATION RESULTS

Separation of methane from a mixture of CH_4/N_2 was studied by using the four-step PSA cycle, Cycle 1. A similar PSA cycle was used for the separation of the H_2/CH_4 mixture (*10, 11*) and the CH_4/CO_2 mixture (*13*).

The total cycle time was 8 min, which constituted four equal time steps. The composition of the gases produced in enhanced recovery projects varies with time. The concentration of CH_4 in these projects starts with approximately 90% and decreases with time to about 30% (*1*). This decrease in CH_4 concentration occurs over a period of several years. For simulation purposes, however, a feed composition of 50/50 CH_4/N_2 is used.

The bed characteristics along with other model input parameters are listed in Table 2. For a given bed and total cycle time, the important process variables are feed rate, high pressure, low pressure, pressurization mode, and CH_4 purge to feed ratio. Methane purge to feed ratio is defined as the ratio of moles of CH_4 input in Step III to the moles of CH_4 in th feed. The effects of feed rate, high and low pressures, and mode of pressurization have been discussed earlier (*8, 18*). In this study we present the effect of a high pressure heavy component purge on separation performance. Also, a comparison is given between three PSA cycles which differ mainly in Step III.

TABLE 2
Adsorption Bed Characteristics and Langmuir Isotherm Parameters

Bed length: 500 cm
Bed diameter: 100 cm
Total void fraction: 0.73
Interparticle void fraction: 0.43
Bed density: 0.4 g/cm^3
Heat capacity of adsorbent: 0.25 cal/g/K
Heat of adsorption of methane: 4.846 kcal/mol
Heat of adsorption of nitrogen: 2.463 kcal/mol
Heat capacity of methane: 8.54 cal/mol/K
Heat capacity of nitrogen: 6.51 cal/mol/K

Langmuir isotherm[a] parameters at 298 K:

CH_4: $q_m = 8.423 \times 10^{-3}$ mol/g
$b = 8.43 \times 10^{-2}$ 1/atm

N_2: $q_m = 3.208 \times 10^{-3}$ mol/g
$b = 6.42 \times 10^{-2}$ 1/atm

[a] $q = q_m bP/(1 + bP)$.

Effect of CH_4 Purge

The PSA cycle used here involves a high pressure methane purge. As suggested earlier (*12*), the purpose of this step is to increase the fraction of CH_4 remaining in the bed at the end of the step, so that a high purity CH_4 product can be obtained. The function of this step was studied further by varying the CH_4 purge to feed ratio. The CH_4 purge to feed ratio is defined as

$$CH_4 \text{ purge/feed} = \frac{\text{amount of } CH_4 \text{ used in Step III}}{\text{amount of } CH_4 \text{ in feed in Step II}}$$

Three runs at 0.5, 1.0, and 1.5 CH_4 P/F ratio showing the effects of the CH_4 P/F ratio on separation performance are given in Table 3 and Fig. 7. The other operating conditions were kept the same for the three runs. It is seen that increasing the CH_4 P/F ratio from 0.5 to 1.0 increases the CH_4 product purity without affecting the product recovery significantly. However, a further increase in the CH_4 P/F ratio increases the CH_4 product purity at the expense of a significant drop in CH_4 product recovery. Thus,

TABLE 3
Cyclic Steady-State Results of PSA Separation of a 50/50 CH_4/N_2 Mixture at Various Operating Conditions[a]

Run no.	CH_4 P/F ratio	P_{III} (atm)	Separation results			
			CH_4 product purity (mol%)	CH_4 recovery (%)	N_2 product purity (mol%)	N_2 recovery (%)
1	0.5	—	80.727	78.287	92.103	73.633
2	1.0	—	90.732	73.825	88.277	85.827
3	1.5	—	99.217	58.167	84.790	94.756
4	—	1.5	77.717	91.170	96.184	68.405
5	—	1.0	83.760	73.392	87.602	79.568
6	—	0.5	91.696	47.135	78.655	89.331
7	0.5	1.5	88.032	75.041	89.733	81.017
8	0.5	1.0	98.429	59.749	84.515	90.019
9	0.5	0.5	99.775	10.046	73.290	94.574

[a] P_H = 2 atm, P_L = 0.01 atm, feed rate = 4.3×10^4 L STP/cycle.

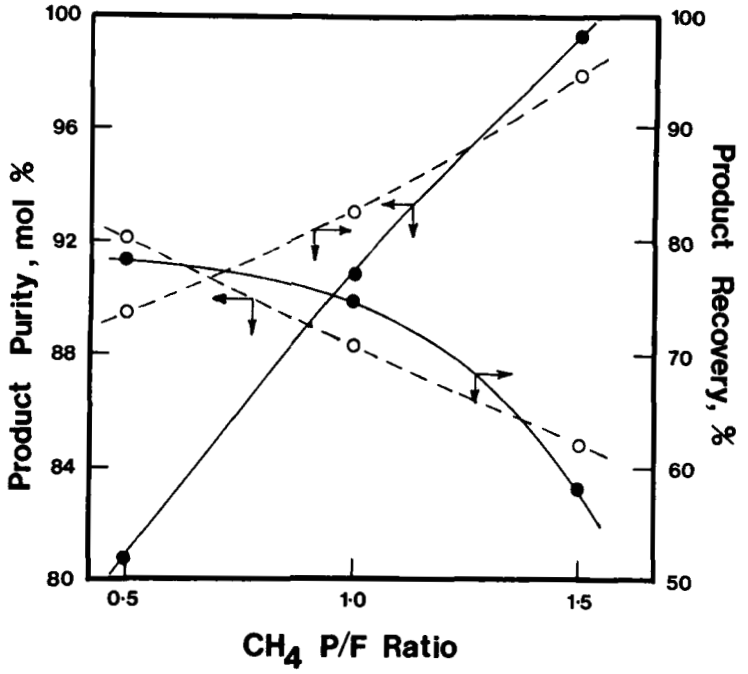

FIG. 7. Effect of CH_4 purge /feed ratio on the separation performance. (●) CH_4 product, (○) N_2 product.

an optimum value of the CH_4 P/F ratio should be used. The function of CH_4 purge is to push the CH_4 concentration wavefront in the bed so as to enrich the bed with CH_4 content at the end of Step III, keeping the wavefront sharp. Figure 8 shows the bed concentration profiles at the end of Steps II, III, and IV for three different CH_4 P/F ratios. It should be noted that in this analysis the average concentration of the Step IV effluent is used as the concentration of CH_4 purge, and pressurization is accomplished by the average Step II N_2 product, which was not the case in earlier studies (*11, 12*). From Fig. 8 it is seen that the bed concentration profiles at the end of Step IV are nearly identical because the same low pressure, P_L was used in all three runs. Also, the profiles at the end of Step II, the feed step, are similar. The wavefront reaches approximately 0.9 L from the feed end of the bed at the end of Step II, and the bed is saturated with feed, 50/50 N_2/CH_4 mixture, behind this wavefront. In Step III another wavefront

travels through the bed. The CH_4 concentration behind this wavefront is the average concentration of the Step IV CH_4 product. For CH_4 P/F = 0.5 (see Fig. 8), the latter wave has traveled approximately 40% of the bed, pushing the former wave out of the bed. As the CH_4 P/F ratio is increased to 1.0, the latter wave travels through 75% the bed at the end of Step III, thus increasing the CH_4 concentration in the bed significantly and not losing much more CH_4 in the N_2 product. However, for CH_4 P/F = 1.5 the latter wavefront also breaks through the bed at the end of Step III, which reduces the CH_4 recovery significantly. Thus, for a high purity CH_4 product the CH_4 P/F ratio should be chosen such that the latter wave travels through the bed without breaking through, which will result in higher purity without lowering the recovery much.

Comparison of Different PSA Cycles

Many different PSA cycles have been reported in the literature (*4, 12*) which differ in the depressurization steps. The commonly used depressurization step consists of cocurrent blowdown followed by countercurrent depressurization. The purpose of cocurrent blowdown is to recover the light component remaining in the voids, thus increasing the recovery of light component product and purity of heavy component product. A cycle involving cocurrent blowdown step was used here for comparison. This cycle consists of the following steps:

Step I:	N_2 product pressurization
Step II:	High pressure adsorption
Step III:	Cocurrent blowdown
Step IV:	Countercurrent evacuation

The total cycle time was 8 min and consisted of 4 equal time steps. This cycle will be referred to as Cycle 2.

During the cocurrent blowdown step, the heavy component wavefront becomes diffused because of a decrease in pressure. Although this step allows some of the light component remaining in the voids to be recovered, it does not allow a very efficient separation during this step because of the diffused wavefront. This problem is circumvented by using a heavy component purge at feed pressure. However, as the heavy component is obtained at low pressure, it needs to be pressurized to high pressure to be used as a heavy component purge. This results in additional cost.

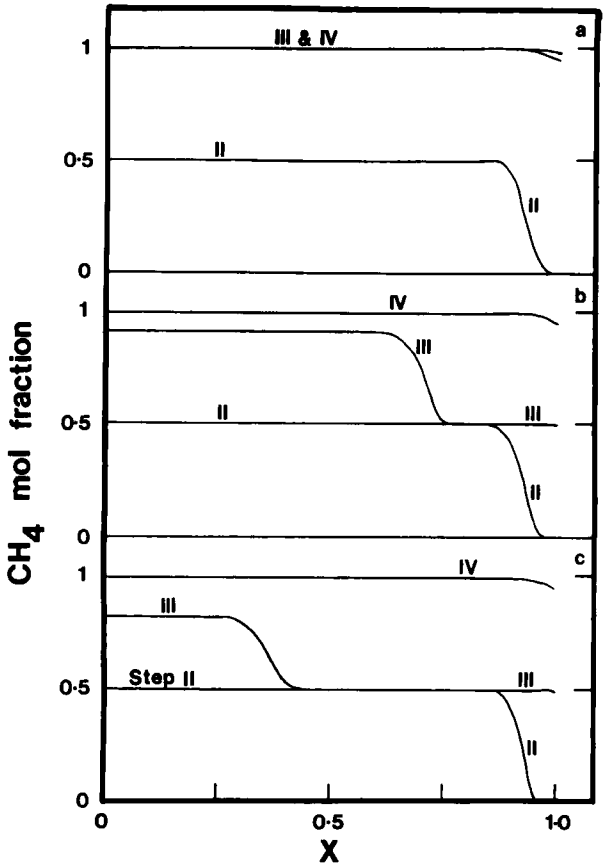

FIG. 8. Bed concentration profiles at the end of Steps II, III, and IV: Effect of CH_4 purge/feed ratio. (a) CH_4 P/F = 1.5, (b) CH_4 P/F = 1.0, and (c) CH_4 P/F = 0.5.

A new cycle is suggested in which Step III is an integrated step involving cocurrent blowdown and heavy component purge. This cycle consists of Steps I, II, and IV similar to those of Cycle 1 and Cycle 2. Step III, however, is divided into two steps:

Step IIIa: Cocurrent blowdown
Step IIIb: Heavy component purge

This cycle will be referred to as Cycle 3. The cycle time for Cycle 3 was 8 min, consisting of three steps (Steps I, II, and IV) of 2 min each and two steps (Steps IIIa and IIIb) of 1 min each. In this cycle the pressure is reduced to some intermediate pressure (P_I) in Step IIIa, and the heavy component purge is achieved at P_I. This reduces the cost of pressurizing a part of the heavy component product, and gives enough time in Step IIIb to sharpen the heavy component wavefront.

Cycles 1 to 3 are compared in Table 3. It has been suggested that different PSA cycles should be compared based on their performance curves (*12, 18*). A performance curve is defined as the relationship between product purity and product recovery at a given throughput, high pressure, and low pressure. For Cycle 1 a performance curve was obtained by varying the CH_4 P/F ratio, whereas for Cycle 2 the end pressure of cocurrent blowdown was varied. For Cycle 3, either cocurrent blowdown end pressure or the CH_4 P/F ratio can be varied to obtain a performance curve. In this study, cocurrent blowdown end pressure was varied while keeping the CH_4 P/F ratio fixed. The performance curves for the three cycles are compared in Fig. 9. A higher curve corresponds to a better separation performance for that component. From Fig. 9 it is seen that Cycle 1 is better than Cycle 2 if CH_4 is the desired product. However, for high purity N_2 product, Cycle 2 shows a better separation performance. The performance of Cycle 3 lies between those of Cycles 1 and 2. It is seen that for CH_4 product the performance of Cycle 3 is comparable to that of Cycle 1, thus suggesting that Cycle 3 is in fact better because it provides savings in pressurization costs.

The differences among the three cycles can be better understood in terms of bed profiles. For comparison, three runs (Runs 2, 5, and 7) were chosen as the three runs with similar CH_4 recoveries. The three runs show CH_4 product recoveries of about 74%. The bed concentration profiles for the three runs are shown in Fig. 10. The bed concentration profiles at the ends of Steps I, II, and IV are nearly identical. The main differences occur in Step III. In Cycle 1 the CH_4 product purge with a concentration of

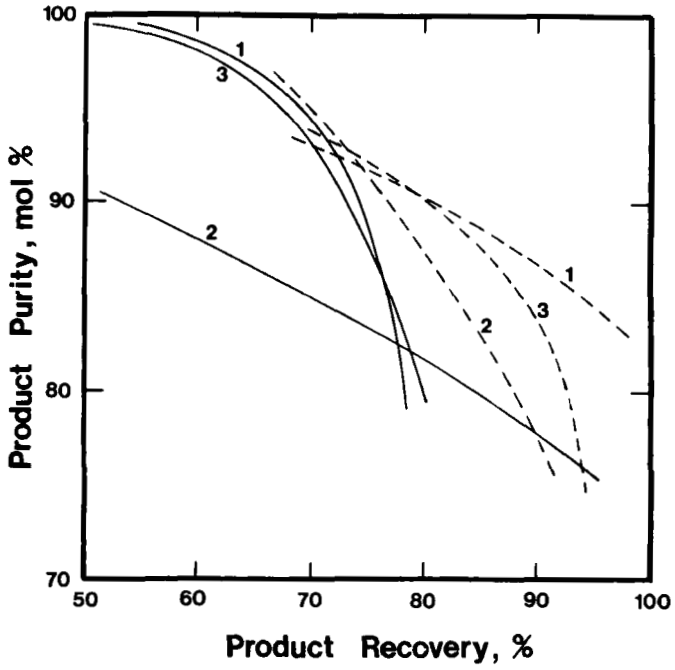

FIG. 9. Comparison of different PSA cycles. The numbers on the curves refer to the cycles. Solid line: CH_4 product. Dashed lines: N_2 product.

90.7% saturates approximately 70% of the bed and gives a sharp wavefront at the end of Step III. In the case of Cycle 2, however, the concentration profile in the bed at the end of Step III is very diffused; the wavefront spans nearly the whole bed with approximately 66% CH_4. This is responsible for a much lower concentration of CH_4 product purity. For Cycle 3 it is seen that at the end of Step IIIa the wavefront is diffused; however, it does not span the whole bed as it did in Cycle 2. Also, the average CH_4 concentration in the bed at the end of Step IIIa is lower than it is at the end of Step III for Cycle 2. Another wavefront travels through the bed, corresponding to Step IIIb. The bed is saturated with a gas mixture containing approximately 88% CH_4 behind this wavefront. On comparison, it is seen that the purity of the CH_4 product from Cycle 3 lies between those of Cycles 1 and 2.

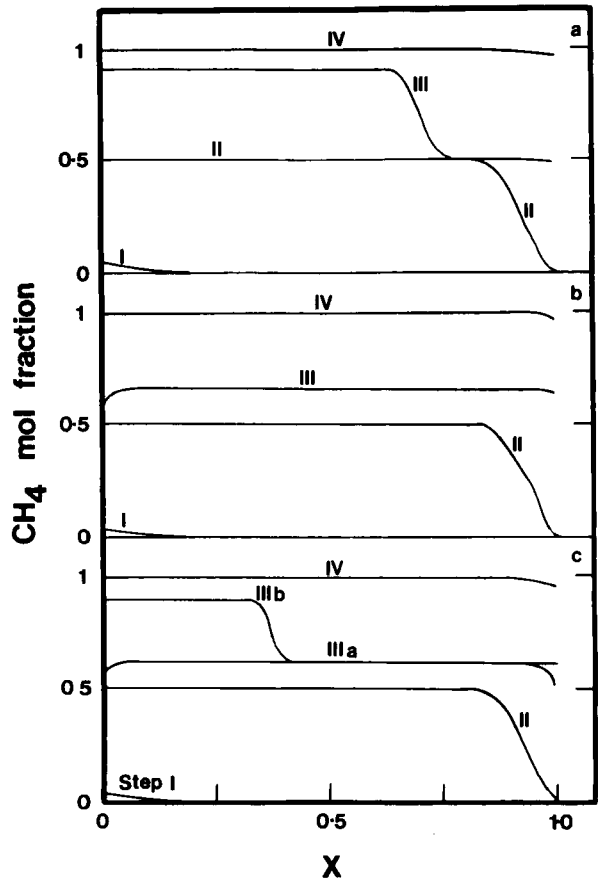

FIG. 10. Bed concentration profiles at the end of different PSA cycle steps: Comparison of different PSA cycles. (a) Cycle 1, (b) Cycle 2, and (c) Cycle 3.

Comparison with Other PSA Processes for the Separation of CH_4/N_2 Mixture

In the past, molecular sieve 5A (*19*) and zeolite clinoptilolite (*20*) have been used for the separation of CH_4/N_2 mixtures. In molecular sieve 5A, separation is achieved due to equilibrium selectivity, whereas for zeolite clinoptilolite separation is due to the difference in the diffusion rates of CH_4 and N_2 into the adsorbent, i.e., N_2 diffuses faster than CH_4. Thus, by controlling the cycle time, N_2 is preferentially adsorbed on clinoptilolite.

Frankiewicz and Donnelly (*20*) studied the effects of high pressure, regeneration time, temperature,and particle size on the separation of a 60/40 CH_4/N_2 mixture on clinoptilolite by using a three-point factorial design. The authors presented the separation results in the form of the average amount of N_2 adsorbed per gram adsorbent per cycle and the separation factor. Product purity and recovery were calculated from these results. The experiments were performed in the 140–250 L STP/h/kg and 75–150 psia ranges. The maximum CH_4 product purity reported in their study was 87%. For the CH_4 product to be commercially useful as pipeline gas, it should be 90%. Due to the lack of data on clinoptilolite, a comparison of the separation results cannot be made based on the performance curves. Also, the pressure range used on clinoptilolite is much higher than the pressure range used in the present study. Nevertheless, a comparison between the results of the two studies is shown in Fig. 11. It is seen that in the range of CH_4 product purities that can be compared, clinoptilolite gives comparable product recoveries, although it should be noted that the feed composition used for clinoptilolite contained 60% CH_4 compared to 50% in the present study.

Molecular sieve 5A was used for the separation of a 71.4/28.6 CH_4/N_2 mixture by using a rapid pressure swing cycle (*19*) with the cycle time in the range of 2.5 to 20 s. Due to the lack of data, the feed throughput could not be calculated. Three typical experimental separation results on molecular sieve obtained at 30 psia have been compared with the results obtained in the present study in Fig. 11. It is seen that the maximum CH_4 product purity reported (*19*) is less than 90%. Again, it is seen that in the range of product purity that can be compared, the two adsorbents give comparable separation performance, although the results on molecular sieve 5A are slightly better. Again, the feed used for the molecular sieve 5A study contained 71.4% CH_4 compared to 50% in the present study.

The comparison given in Fig. 11 shows that the process studied in this

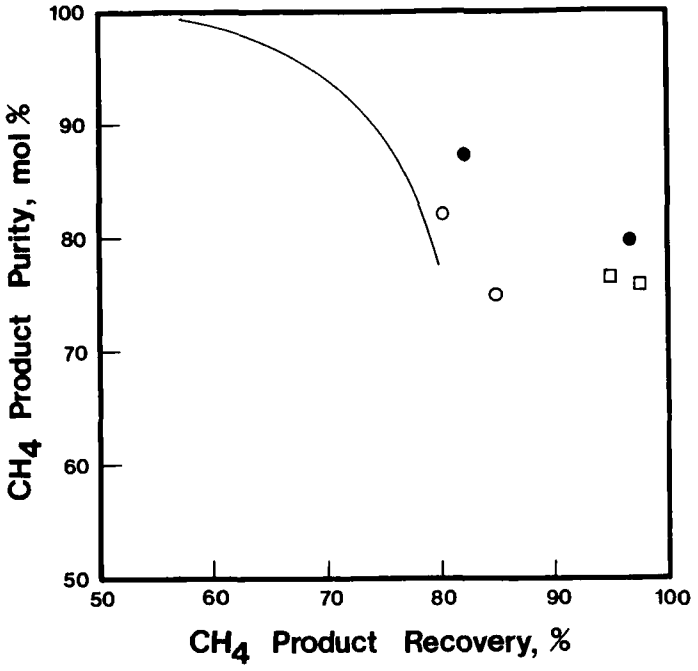

FIG. 11. Comparison of PSA processes using different adsorbents. (□) Feed 71.4/28.6 CH_4/N_2, 30 psia (*19*). (●) Feed 60/40 CH_4/N_2, 142.7 L STP/h/kg (*20*). (○) Feed 60/40 CH_4/N_2, 249.7 L STP/h/kg (*20*).

work can give high purity CH_4 product at high recovery and throughput. However, it is difficult to make an ultimate comparison of different processes because the results presented on other adsorbents as well as the results obtained in this study may not be at the optimum conditions. Also, the ultimate comparison would have to include economic considerations that were not considered in the present study.

Acknowledgment

We acknowledge support by the donors to the Petroleum Research Fund administered by the American Chemical Society.

NOMENCLATURE

b, q_m	Langmuir isotherm parameters (see Table 2)
C	gas-phase concentration
P	pressure
PSA	pressure swing adsorption
q_i	amount adsorbed of Component i
q_i^*	amount adsorbed at equilibrium
T	temperature
t	time
u	interstitial velocity
x	dimensionless length of bed
X_i	mole fraction of Component i in the adsorbed phase
Y_i	mole fraction of Component i in the gas phase
Z	axial position in the bed

Subscripts

f	feed
g	gas
H	high
L	low
i	Component i
0	ambient or initial condition
Pr	pressurization
Pu	purge
III	end of Step III (Cycle 2)
I	end of Step IIIa (Cycle 3)

REFERENCES

1. H. L. Vines, *Chem. Eng. Prog., 11,* 46 (1986).
2. A. Wennerberg and T. O'Grady, U.S. Patent 4,082,694 (1978).
3. *National Bureau of Standards (U.S.), Monograph 25,* October 1981, Section 18, page 44.
4. R. T. Yang, *Gas Separation by Adsorption Processes,* Butterworths, Boston, 1987.
5. D. Tondeur and P. C. Wankat, *Sep. Purif. Methods, 14*(2), 157 (1985).

6. S. Sircar, in *Adsorption: Science and Technology* (A. E. Rodrigues, M. D. LeVan, and D. Tondeur, eds.), Kluwer, Boston, 1989, p. 285.
7. C. W. Skarstorm, *Ann. N. Y. Acad. Sci., 72,* 751 (1959).
8. A. Kapoor and R. T. Yang, *Sep. Sci. Technol., 23*(1-3), 153 (1988).
9. P. L. Cen and R. T. Yang, *Ibid., 20,* 725 (1985).
10. R. T. Yang and S. J. Doong, *AIChE J., 31,* 1829 (1985).
11. P. L. Cen and R. T. Yang, *Sep. Sci. Technol., 21*(9), 845 (1986).
12. S. J. Doong and R. T. Yang, *Chem. Eng. Commun., 54,* 61 (1987).
13. S. Sircar, *Sep. Sci. Technol., 23*(6-7), 519 (1988).
14. T. Tamura, U.S. Patent 3,797,201 (1974).
15. S. Sircar and J. W. Zondlo, U.S. Patent 4,013,429 (1977).
16. S. J. Doong and R. T. Yang, *React. Polym. 6,* 7 (1987).
17. A. Kapoor and R. T. Yang, *Ind. Eng. Chem., Res., 27,* 204 (1988).
18. A. Kapoor and R. T. Yang, *Chem. Eng. Sci., 44*(8), 1723 (1989).
19. P. H. Turnock and R. H. Kadlec, *AIChE J., 17*(2), 335 (1971).
20. T. C. Frankiewicz and R. G. Donnelly, in *Industrial Gas Separations* (T. E. Whyte Jr., C. M. Yon, and E. H. Wagner, eds.), American Chemical Society, Washington, D.C., 1983.

Received by editor August 14, 1989